J. Membrane Biol. 88, 33–43 (1985)

The Journal of
Membrane Biology

Intercellular Fibrillar Skeleton in the Basal Interdigitations of Kidney Tubular Cells

G. Zampighi and M. Kreman
Department of Anatomy and Jerry Lewis Neuromuscular Research Center, UCLA School of Medicine, Los Angeles, California 90024

Summary. The tubular cells from the thick ascending limb of the loop of Henle in rabbit kidney medulla contain in their basal-lateral surfaces a complex system of interdigitations. Within these interdigitations, the plasma membranes are separated by extracellular spaces of relatively constant width that contain a previously undescribed fibrillar system. The structural organization and distribution of this intercellular fibrillar skeleton was studied using freeze-fracture etch and then section electron microscopy. The skeleton is comprised of discrete strands with a density of 300 to 400 per μm^2 evenly distributed along the entire basal-lateral region. Each strand has the shape of a brace and it is constructed from up to eight finer filaments each having a width of about 2 nm. The filaments are tightly joined together along their shafts for about 30 nm but they separate at both ends for about 10 nm before contacting the external surface of the plasma membrane. We propose that this intercellular fibrillar skeleton is responsible for maintaining the wide (about 50 nm) and uniform plasma membrane separation along the entire length of the basal-lateral region of the tubular cells of the thick ascending limb.

Key Words plasma membrane connections · kidney loop of Henle

Introduction

A striking characteristic of the organization of the cells of many epithelia functioning in active transport of cations is a highly organized system of plasma membrane interdigitations that form a labyrinth of intercellular spaces in their baso-lateral surfaces [1, 15]. In mammalian kidney, these interdigitations are seen in the proximal convoluted tubules [20–21], the thick ascending limb of the loop of Henle [16–18], the distal tubule [16–18] and portions of the collecting duct [15, 16]. In kidney tubules, these interdigitations are characterized by the presence of an extracellular space of relatively constant width (about 50 nm), separating the parallel membranes of adjacent cells. This wide (about 50 nm) and uniform separation between the plasma membranes would be difficult to explain without the assumption of an intercellular skeleton of precise architecture. This is because the separation between membranes is too wide for the attractive Van der Waals interaction to be important. However, indications of an intercellular skeleton have not been obtained in several electron-microscopic studies of the renal tubules (4, 12–17, 20, 21). By using freeze-fracture methods followed by sublimation of layers of water of controlled thickness on the fractured surface, an organized intercellular system composed of strands that span the extracellular gap and attach to the plasma membranes was uncovered.

Materials and Methods

In all studies, kidneys obtained from 9- to 10-week-old rabbits (Kurd's Caviary Animal Supply) were used. The kidneys were bisected along their long axis, and thin strips of the outer medulla were excised from the organ.

Preparation of the Tissue for Freezing

In this study, we used both fixed and unfixed tissue. For the unfixed specimens, the thin strips of outer medulla were further trimmed to a standard volume (hereafter called blocks) of about $0.25 \times 0.25 \times 0.5$ mm^3. These blocks were placed on Balzers specimen holders and frozen by immersion in liquid propane (Air Products and Chemicals, Inc., Tamaqua, Pa.) using a guillotine-type device [2]. The tissue was frozen in its own "natural juices."

For fixed specimens, the strips of outer medulla were fixed in 4% glutaraldehyde in 0.2 M sodium cacodylate, pH 7.4, for 1 hr at room temperature. After fixation, the strips were further trimmed to the standard blocks and then washed extensively in distilled water. The blocks were then placed on Balzers holders, carrying with them a minimum amount of water whereupon they were equilibrated in a chamber equilibrated at 100% relative humidity. Empirically it was found out that 3 to 5 min of incubation removed most of the excess water without drying the tissue. A dried piece of tissue can easily be recognized because the tissue

darkens and does not adhere properly to the block, with the result that it is usually knocked off the holder during fracturing. The holders containing the tissue were frozen in liquid propane as for the unfixed samples.

Freezing Methods

The preservation of a microscopic structure during freezing is inversely related to the final dimensions of the ice crystals that form. Ideally, one would like to freeze and maintain the water in its solid amorphous state during the entire procedure. In freeze-fracture-etch technique, however, crystalline ice is necessarily present. Crystals of ice are produced during two steps of the preparation of the specimen. The first is during freezing. The size of the crystals of water obtained during this step can be minimized by using small pieces of tissue and keeping the amount of excess water to a minimum with a constant humidity chamber. The second step that results in ice crystal formation occurs when the temperature of the specimen is raised above its devitrification temperature (−140 to −135°C) [3]. Because sublimation (etching) must be performed at temperatures well above the devitrification temperature, ice crystals (of different sizes) are certain to form in the tissue.

We have found that these slight modifications provide details on the surface of membranes of fixed and unfixed samples of kidney medulla frozen by immersion in liquid propane. In addition, it is not necessary to pretreat the tissue with chemical agents such as detergents or cryoprotecting agents such as methanol. Applying these precautions, we found islands of tissue where structural detail are observed deeper into the frozen blocks and not just limited to the outermost surface.

Freeze Etching

Freeze-fracture etch was performed in an Edwards 306 coater and a Balzers 301 (Balzers Co., Nashua, N.H.) apparatus. The holders were transferred from liquid nitrogen to a specimen table cooled to −160°C. After a pressure of about 10^{-6} mbar was reached, the temperature of the specimen table was increased passively to the temperature at which both fracturing and etching were carried out (either −150° or −100°C). This procedure took 10 to 15 min. The tissue was fractured with a knife cooled to liquid nitrogen temperature. Etching was performed by leaving the cold knife over the specimen for 30 sec or 1 min. The surface was replicated unidirectionally at 45° (when using the Edward coater) or rotary shadowed at 25° (when using the Balzers apparatus) with platinum-carbon and at 90° with carbon.

The preservation of the tissue as a function of the position along a 0.25-mm-thick specimen was estimated by using a Balzers cold stage that accommodated several (up to four) samples. Since the cold knife fractures the four specimens at different depths, a given experiment provides a gross sampling of the quality of the freezing along its entire thickness. To our surprise islands of well-preserved tissue were present along the entire thickness (0.25 mm) of the sample. Therefore our strategy was to first prepare with a knife a flat and smooth fracture surface without concern from which region of the specimen it would arise. In these replicas, we then searched for those regions that were frozen without the distortion produced by the large hexagonal ice crystals that are characteristic of the slow frozen regions.

Thin Sectioning

Some of the standard blocks of tissue, fixed in glutaraldehyde and rinsed in distilled water, were processed for thin sectioning according to methods published elewhere [22–24]. Fixation was completed by immersing the pieces of kidney in a solution of 4% glutaraldehyde, 0.5% tannic acid (Sigma Chemical Co., St. Louis, Mo.) in 0.2 M sodium cacodylate buffer, pH 7.3, for 1 hr at room temperature. Postfixation was carried out in 1% osmium tetroxide in 0.2 M cacodylate buffer, pH 7.3. The pieces of kidney were also stained in block by immersing them in a solution containing 0.5% uranyl acetate in 0.1 M sodium acetate buffer, pH 5.0, at 4°C for at least 24 hr. Dehydration was carried out in ethanol and embedding in Epon 812. Sections were cut with a Sorvall MT 5000 ultramicrotome (DuPont Co., Newton, Conn.) and stained on the grids with uranyl acetate and lead citrate.

Electron Microscopy

The microscopy was performed with either a Zeiss 10C and an EM 109 microscope. Stereo-tilted pairs were obtained using the Zeiss high resolution goniometer. The tilt angles used to produce the stereo-pairs were either ±6 or ±12°. We found it convenient to reverse the contrast of the negatives obtained from specimens that were deep etched and rotary shadowed.

Results

Thin Sections

The intercellular spaces in the thick ascending limb of the loop of Henle begin beneath the basement lamina (large arrow, Figs. 1 and 2) and extend deeply into the wall of the tubules until the perinuclear region is reached (Fig. 1). All of the cell mitochondria in each cell are located in the thin slabs of cytoplasm that lie between the intercellular spaces (Figs. 1 and 2). In cross section the intercellular spaces are defined by paired plasma membranes, which in some regions are arranged into ordered stacks (Fig. 2). In these views, the intercellular spaces can be identified by tracing them from their origins beneath the basement membrane (arrow in Fig. 2) into the slots of relatively constant width seen in the cross section. The overall thickness of the complex formed by the two plasma membranes and the intervening space in these specimens ranged from 40 to 53 nm. The intercellular space contained material organized as dense granules arranged in rows, equidistant from the two external surfaces. In some instances, these granules are found evenly spaced at distances 35 to 40 nm apart (Fig. 2, arrowheads). However, inspection of a large number of micrographs from different viewing angles, did not indicate a periodic organization of

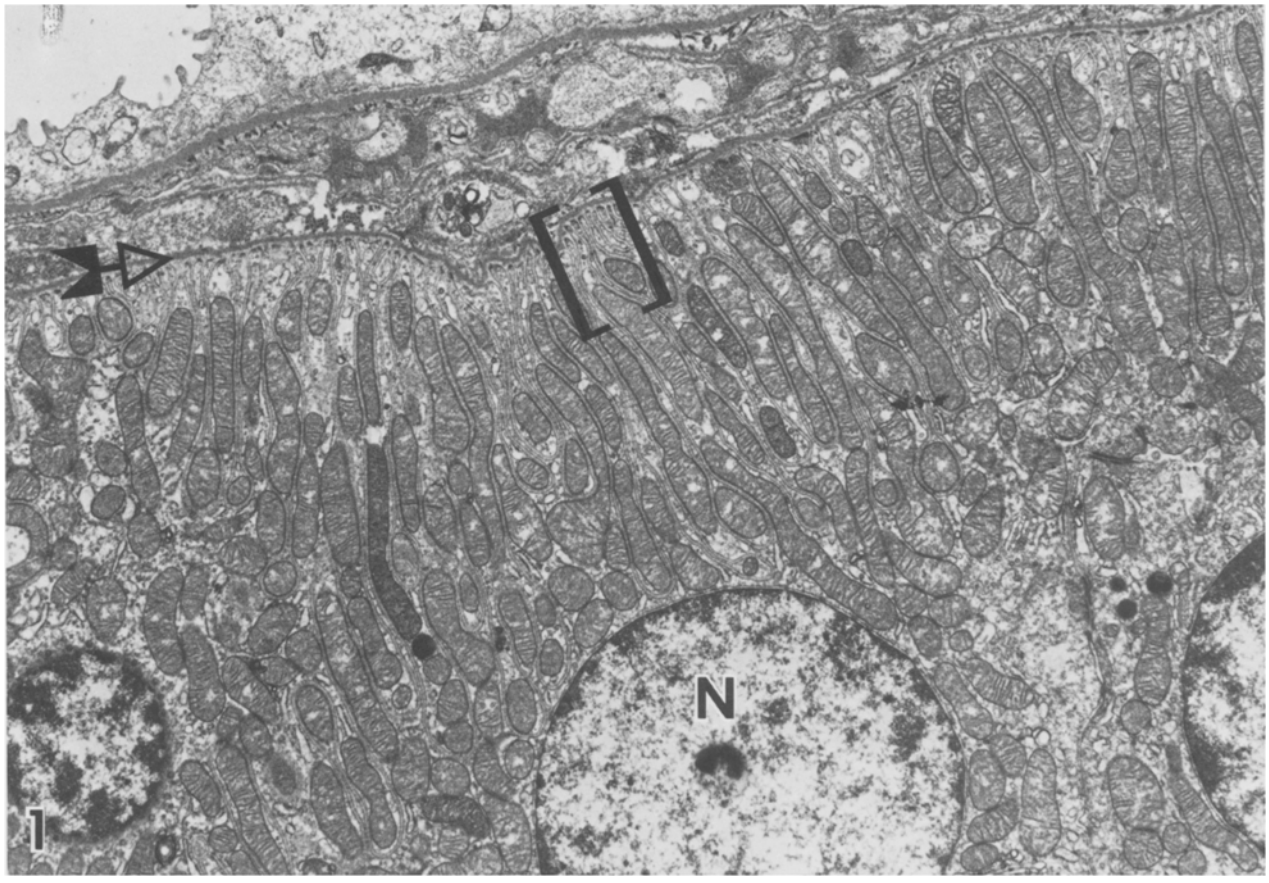

Fig. 1. Low magnification view of a thin section of the basal-lateral region of the thick ascending limb of Henle's loop. The basement lamina (large arrow) is separated by a clear space from the tips of the plasma membrane interdigitations which extend deep inside the cell cytoplasm to the regions around the nucleus (*N*). Note the extent and complexity of the membrane specializations as well as the abundance of mitochondria. A region as that inside the brackets is presented at higher magnification in Fig. 2. Magnification: 7,500×

the intercellular granules. At higher magnification it can be seen that the spaces containing electron-dense material communicate freely with the extracellular space beneath the basal lamina of the tubule (Fig. 2, open arrows). Note that the spaces separating the external plasma membrane surfaces have a uniform width along extensive regions whereas the spaces separating the cytoplasmic surfaces are highly variable in width.

Freeze-Fracture Etch

To obtain additional information about the detailed organization of the elements within the intercellular spaces, the technique of freeze-fracture etch followed by unidirectional shadowing was utilized. The process of sublimation, etching, at high vacuum could introduce artifacts in the preservation of the material located at the intercellular spaces. Therefore, we performed experiments in which the thickness of the layer of water sublimed was increased systematically.

In a replica of a fractured surface from which only a thin layer of water has been sublimed (Fig. 3), intercellular spaces that have been fractured either transversely or slightly obliquely clearly display views similar to those presented in the sectioned tissue (Fig. 2). In this figure, the gap observed between the membranes which compose the infoldings shown in Fig. 3, is significantly larger than usual (about 70 nm). This increase in the width of the extracellular gap is probably due to the wash with distilled water that is performed after glutaraldehyde fixation and prior to freezing. Measurements of the overall width of intercellular spaces obtained from specimens that had been frozen unfixed and uncryoprotected yielded an average value

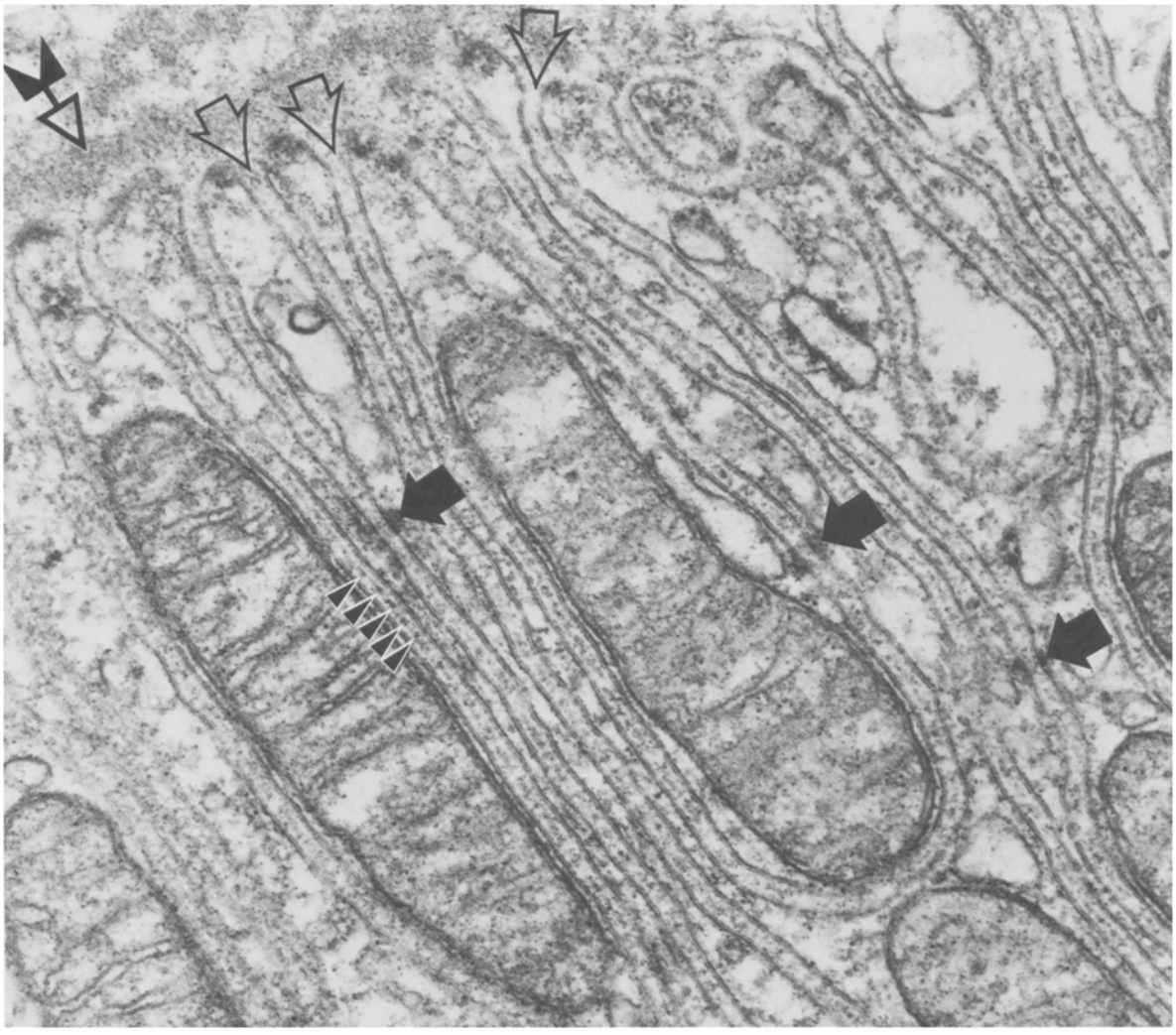

Fig. 2. A higher magnification view of the basal region of the cell just beneath the basement lamina (large arrow). This figure shows that the interdigitations stack into bodies of parallel plasma membranes separated by extracellular and cytoplasmic spaces. The distinction among these spaces is made easy because the intercellular space can be traced from the tips of the interdigitations (open arrows) to regions deep inside the cytoplasm. The intercellular spaces are of constant width and contain dense particles that, at places, are regularly spaced (arrowheads). Another membrane specialization in this region is a small, desmosome-like junction (solid black arrows) characterized by a smaller width of their extracellular gap and by dense material associated symmetrically to the cytoplasmic leaflets. Magnification: 62,500×

for the separation between the paired membranes of 50 to 55 nm. This value is in good agreement with those observed in thin sections (Figs. 1 and 2) and that reported by Pease [17] for tissue embedded in water-soluble polymers.

The expanded intercellular spaces in Fig. 3 allow a clear view into the organized material connecting both plasma membranes. This is particularly evident with specimens from which a small layer of water has been sublimed (−105°C for 30 sec) from the fractured surface. For example the intercellular space labeled with the star has a smooth, almost featureless appearance along its entire length, but the intercellular spaces located in the center and at the left border of this figure are transversed by thin bridges. Some of these bridges only partially traverse the space (straight arrows) while others completely span the space and cast long shadows over the underlying surface of the ice. The smooth appearance of the surface of the ice in this micrograph indicates that the crystals of ice should be smaller than the resolution of the replicating film, even though in this particular replica the fracture penetrated deeply into the tissue (at about half of the thickness of the block).

The information obtained by light etching and

Fig. 3. Freeze-fracture-etch preparation of kidney outer medulla fixed with glutaraldehyde, etched for 30 sec at −105°C and replicated unidirectionally. The paired membranes fractured transversally arise from the convoluted interdigitations of the basal-lateral region. The intercellular space labeled by the star shows a smooth almost featureless surface relief. However, other regions of these paired membranes show distinct bridges spanning the intercellular space. Some bridges seem to cross the space between membranes only partially (arrows) whereas others span the entire space between the plasma membranes. The two curved arrows label a region where both plasma membranes are closely apposed as in tight junctions. Magnification: 75,000×

unidirectional shadowing strongly suggested that material shaped as strands is present in the intercellular space. Moreover, these strands are revealed, partially or totally, depending on the amount of water sublimed. However, these data do not provide information about their fine organization. Such information can be obtained by subliming a relatively thick layer of water (0.1 to 0.15 μm) from the frac-

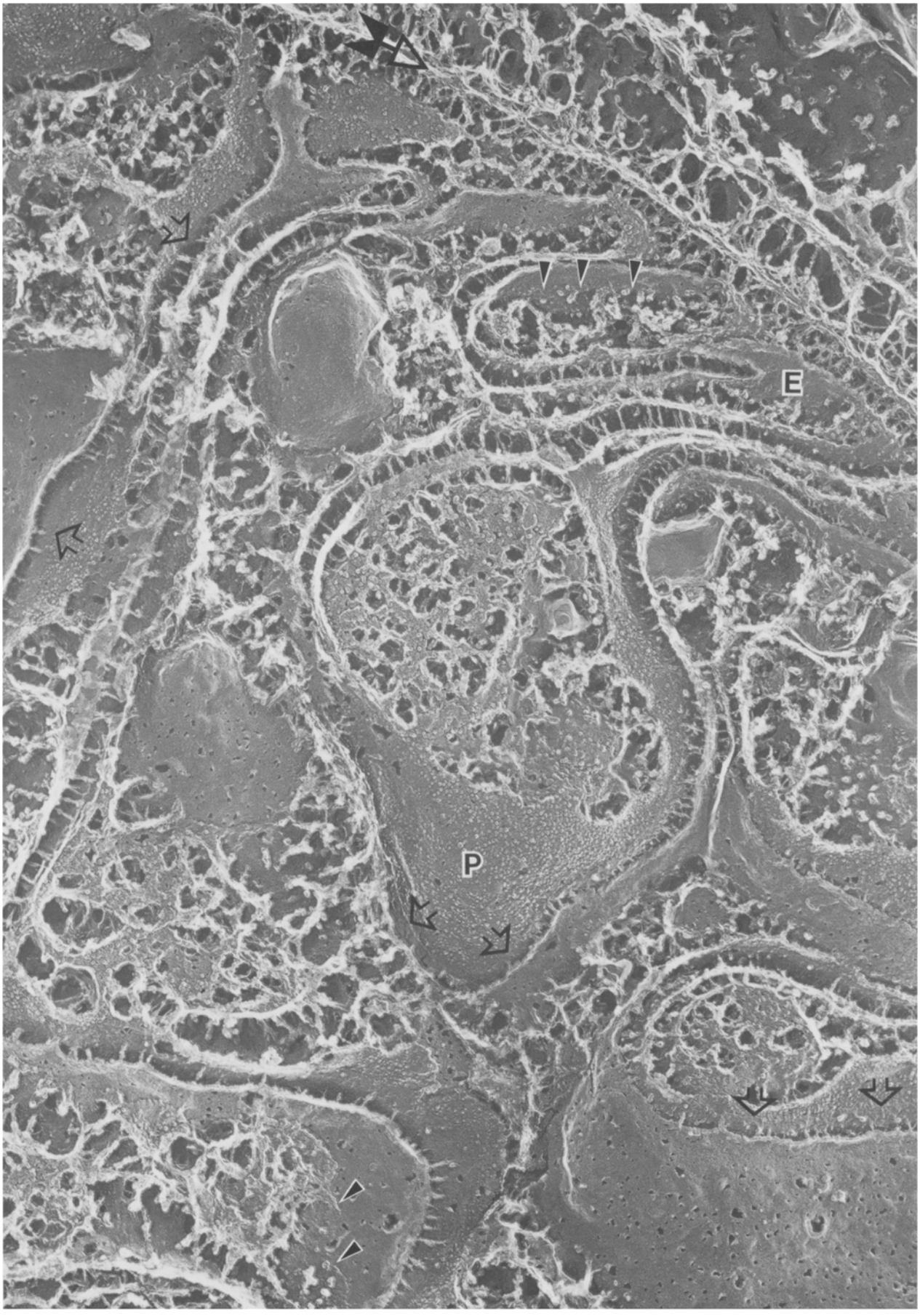
E
P

tured surface followed by rotary shadowing, a technique pioneered by Heuser and Salpeter [10] and extended to many systems by Heuser and collaborators [5–11, 19]. A view of a large region of the basal end of a tubule prepared in this way is presented in Fig. 4. Here the basement lamina (large arrow at the top) can be clearly recognized because of its precise relationship with the tips of the membrane folds that form the intercellular spaces (*compare* Fig. 4 with Fig. 1*A*). In thin sections (Figs. 1 and 2) the basement lamina and the tips of the interdigitations are separated by a clear gap of 70 to 80 nm wide. Freeze-fracture etch followed by rotary shadowing, however, indicates that this gap is not empty but rather contains an anchoring apparatus of complex geometry that connects the basement membrane and the basal plasma membrane of the cell. The network is comprised of numerous strands of variable diameter that branch in all directions. It is surprising that such an elaborate and prominent anchoring apparatus was not detected in conventional thin sections and points out the necessity of looking at cells with more than one method.

Beneath the anchoring apparatus, between the tips of the basal interdigitations of the plasma membrane and the basement membrane, there are several intercellular spaces that can be traced, without interruptions, deeply into the cytoplasm. When intercellular spaces are fractured at different angles, they expose the fractured and etched surfaces of the two membranes that define them. The P fracture face can be recognized in the center of the field because of the presence of numerous annular-shaped intramembrane particles. The P fracture face at the center of Fig. 4 is separated from the true extracellular surface of the membrane by a well-defined fracture step that is labeled at several places with short open arrows. Also visible is the fracture step (closed arrowheads) separating the E fracture face from the true cytoplasmic surface exposed by the evaporation of a layer of water. In this case the fracture step separates the perfectly smooth E fracture face from the etched surface that contains globules of variable size and shape and short bridges that accumulate the metal. Sometimes the bridges located on the true cytoplasmic surface connect to round vesicles.

A prominent feature seen in Fig. 4 is the system of braces located between the pairs of membranes that bridge the intercellular spaces. Because both fractured and etched surfaces were unequivocally identified, these braces can be localized to the extracellular space. There are numerous braces evenly distributed traversing the intercellular spaces with a density of 300 to 400 per μm^2. The braces are about 5 nm in diameter, and usually splay before attaching to the external surfaces of the membranes. Organized material was also observed in the intercellular spaces in thin sections (*see* Fig. 2) and probably it corresponds to the braces that are so prominently arranged in Fig. 4. Thin sections display the globular densities located in the center of the extracellular space, whereas freeze-fracture etch shows columns connecting both external surfaces. Why both techniques show presumably the same type of connections having different appearance will become clear when the fine structure of each brace is considered.

Several views of intercellular spaces containing braces connecting adjacent plasma membranes are presented in Fig. 5 where finer structural features of the braces can be observed. One noteworthy feature is that the widths of the braces are variable. Some of them are thin (about 50 nm), whereas others have widths several times greater. Another feature is that frequently they splay in the region closest to the surfaces of the plasma membranes. Also, when the angles of viewing and shadowing allow lateral views of the braces, one gets the impression that these connections do not appear to be simple circular cylinders but that they are deeper than they are wide.

A stereo-pair of a small portion of an intercellular space that contains several braces is presented in Fig. 6. The brace labeled with the arrowhead strongly suggests the presence of filamental subunits that splay at both ends to contact the surface of the membrane. The brace labeled by a double arrowhead in Fig. 6 has several filaments extending for variable distances along the membrane surface. The two ends of a brace that protrude into the intercellular space may represent structures broken in the fracturing process or the formation or degradation of fully spanned braces.

Fig. 4. Deep-etching followed by rotary shadowing of the basal region of the distal tubule. The specimen was glutaraldehyde fixed, frozen in liquid propane, and etched for 1 min at −100°C. The prominent basement lamina (large arrow) is connected to the tips of the interdigitations through a dense arrangement of interconnecting fibrillar material. Several interdigitations were fractured obliquely and they can be followed deep inside the cytoplasm. Between the paired membranes, a prominent skeleton made up of braces can be observed evenly distributed along the entire length of the interdigitating slabs of cytoplasms. The deep etching performed in this specimen permitted to observe two fracture faces (P and E) and the two etch surfaces. The steps labeled with the open arrows correspond to the separation between the P fracture face and the true external surface. Note that it is on this surface that the braces are located. The arrowheads indicate the step that separates the E fracture face from the true cytoplasmic surface. Magnification: 75,000×

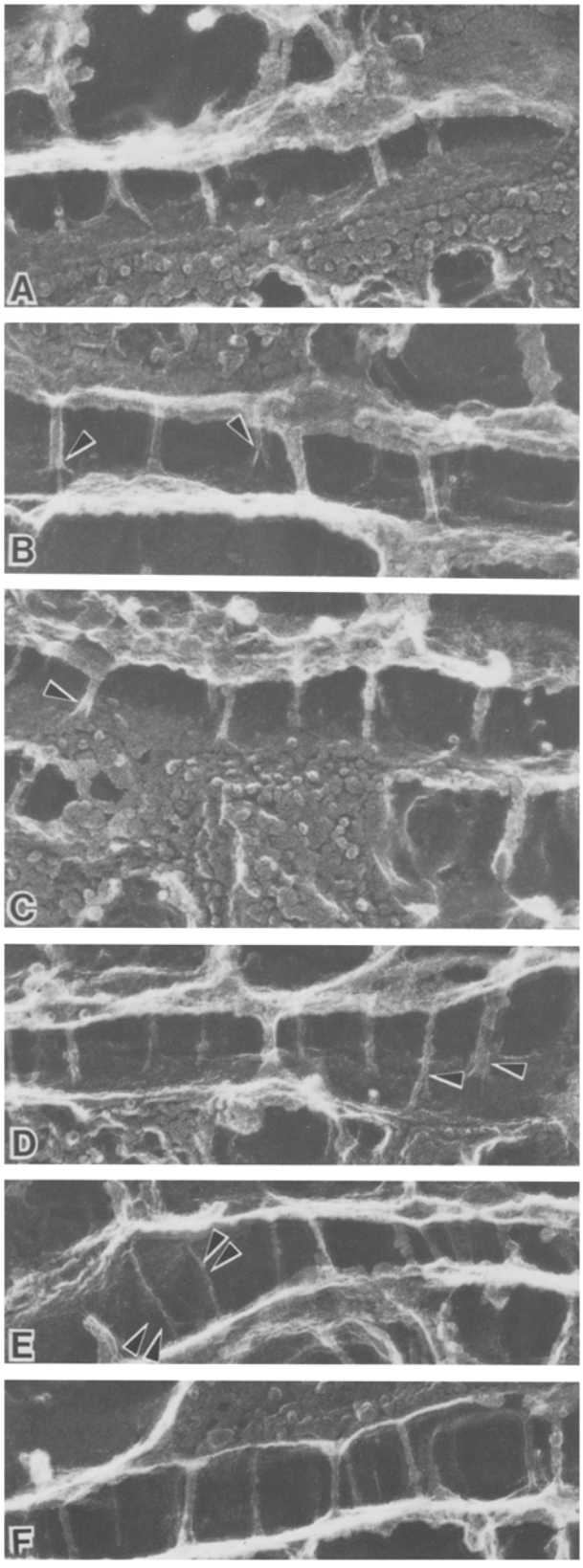

Further structural details of the braces can be obtained by analyzing the higher magnification view of the brace with the arrowhead in Fig. 6 as presented in Fig. 7. This brace has a central element of rectangular shape (10 nm wide and 13 nm thick) without any apparent substructure. The two ends of this brace are about 10 nm long, and they are composed of finer fibrils. The lower end shows three feet that taper when close to the membrane surface. The upper end consists of at least four fine fibrils about 2 nm wide. These fibrils splay at the ends but they are closely apposed when forming the central region of each strand (about 20 nm).

Discussion

In this paper, we report two independent but closely related findings. One is the first demonstration of a new intercellular skeleton in the interdigitations of the tubular cells of the ascending limb of the loop of Henle that might be responsible for the even spacing of plasma membranes. The other is that a slight modification of the freezing method in which small pieces of unprotected tissue are immersed in liquid propane can provide preservation of fine structural details of renal tubules as that accomplished in other tissues by the method of Heuser and Salpeter [10]. A main difference between this method and the one developed by Heuser and Salpeter [10] is that the regions of well-preserved material seem to be islands located along the entire thickness of the tissue block instead of as a continuous layer on the surface.

The intercellular skeleton we have observed is formed from numerous strands each of which acts as a brace to connect the plasma membranes along the entire length of the basal-lateral interdigitations. These braces, presumably oligomeric protein molecules, are novel structures and therefore the possibility that they are some sort of artifact of the preparative procedures should be addressed. The possibility of artifact seems unlikely, because we have observed material localized in the extracellu-

Fig. 5. Higher magnification views of several braces located in the extracellular space of the basal infoldings. The columns have variable width and frequently separate in regions close to the plasma membrane (arrows). In panel E the columns labeled with double arrows seem to extend deeper inside the extracellular space. Magnification: 147,500×

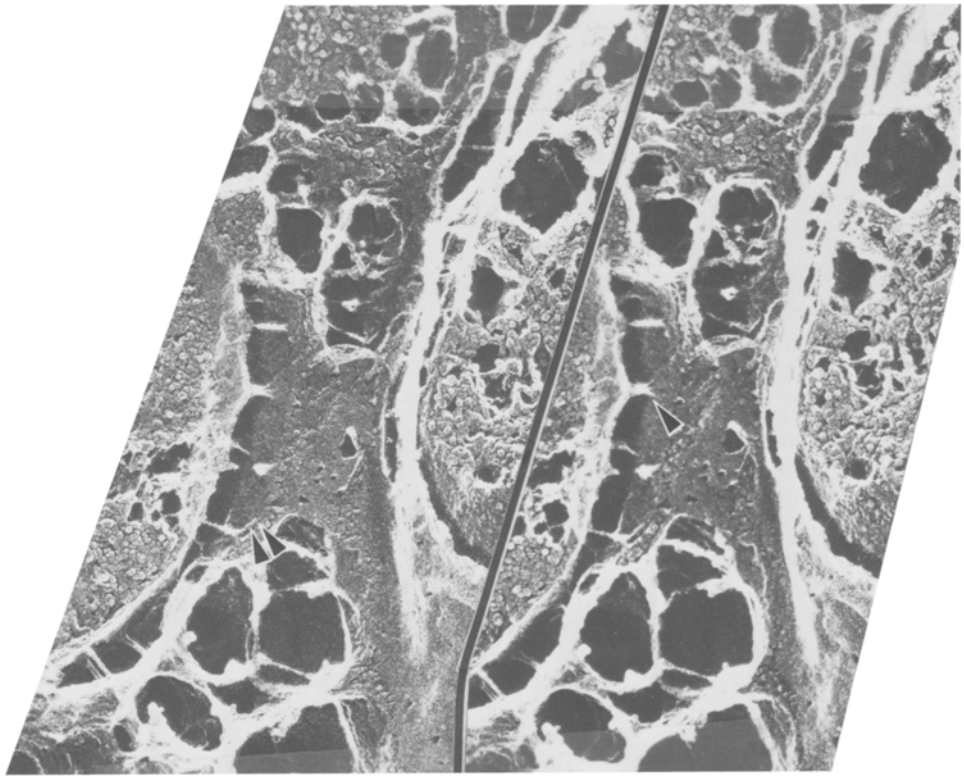

Fig. 6. Stereo-pair of braces contained in the intercellular spaces produced by tilting the replica +6° with respect to the electron beam. The brace labeled with an arrow suggests that it is composed of several thin filaments that are connected along their shafts but they separate close to the membrane surface. The double arrow labels a filament from another brace that extends on the membrane surface. Magnification: 120,000×

lar space (although its appearance and fine details are notably different) by two independent techniques (i.e., freeze-fracture etch and thin sectioning), based on different physical principles. Also, the system of braces was localized along the entire length of the interdigitation, it was absent in the cytoplasm, and it was different from the network observed between the tips of the interdigitations and the basement membrane. More to the point, the braces were seen in all views and increased in frequency as the thickness of the layers of water sublimed during etching was increased. Therefore, their presence do not indicate artifacts peculiar to the rather novel technique of deep etching. All these considerations strongly suggest that an elaborate skeleton of extracellular braces exist within the intercellular spaces of the thick ascending limb of the loop of Henle.

An intercellular fibrillar system with characteristics similar to the one described here was also observed between the lateral surfaces of intestinal epithelial cells by Hirokawa and Heuser [11]. The authors observed narrow strands that bridge the extracellular gap between the plasma membranes. However, they observed these strands most frequently in desmosomes, even though the regions containing them did not display all of the features of desmosomes, such as a smaller overall thickness and the characteristic septum located at the center of the extracellular space. The intercellular skeleton

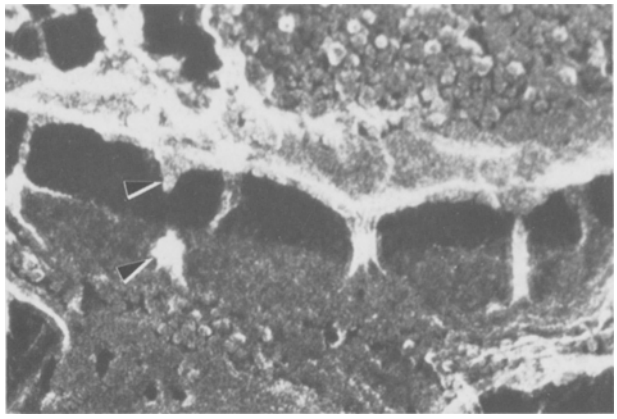

Fig. 7. Higher magnification view of the brace labeled by the arrowhead in Fig. 6. Note that both ends of the strand separate into finer filamentous subunits. This structural feature is well preserved at the upper end of the brace where five filaments can be clearly resolved. The arrowheads label the two ends of a discontinuous brace. Magnification: 277,500×

described here is unequivocally located in the intercellular spaces, and the regions in which it is found are clearly distinguished from the desmosomes in several important features: (i) The overall thickness is almost twice that of a desmosome. (ii) It lacks the symmetric cytoplasmic specializations characteristic of desmosomes. (iii) Small desmosome-like specializations can be seen along the intercellular spaces (Fig. 2) where they can be easily distinguished from the braces.

Our study also provides indications that each brace is made up of several fibrils which interwind in a complicated manner to form each brace. A most characteristic feature of the strands is that the subunits separate at their ends and that spread along the membrane surface probably contacting attachment sites located on the extracytoplasmic surfaces of membrane-bound proteins. To this extent the anchoring mechanism of the braces to the plasma membranes may not require a direct insertion of the braces in the core of the lipid bilayers. Additional support of this anchoring scheme are: (i) the fracture faces of these specialized plasma membranes do not reveal a subset of intramembrane particles reflecting the distribution of the extracellularly located braces. (ii) The braces are not present in highly purified fractions of membrane-bound $(Na^+ + K^+)$-ATPase from the kidney medulla [24]. Moreover, the splaying of the braces into their component filaments might explain why thin sections of the intercellular spaces display globular material located mostly at the center of the extracellular space instead of bridges connecting the membranes. The staining pattern of the centers of the braces must be different from those of the portions where they splay and they should project as dense granules located only at the center of the extracellular gap. This indirect mechanism of anchoring the braces to the membrane surface proposed here would provide a mechanically strong and, at the same time, flexible membrane-membrane interaction that might well serve to keep the width of the extracellular gap within precise limits.

The question naturally arises as to the purpose or physiological relevance of this organelle located at the intercellular spaces of the basal-lateral region of distal renal tubules. The vast interdigitations observed in several regions of the renal tubules have been interpreted as amplifications of the cell surface necessary to accommodate the high density of $(Na^+ + K^+)$-ATPase necessary for active transport [17]. These high concentrations of enzyme are needed for active translocation of cations, which is the primary function of these epithelia. In this regard the braces may insure that the intercellular spaces will have direct and uninterrupted communication with the interstitial space. Should the paired membranes collapse and the intercellular space be compartmentalized into independent lacunae, large regions of the folded membrane will be disconnected from the interstitial fluid. Such a situation would interfere with the efficiency of the transport process. To overcome this difficulty, a passive system of intercellular spacers located between the plasma membranes will keep these channels permanently open to the interstitial fluid.

We wish to thank Drs. J. Kyte and S. A. Simon for their many suggestions and Dr. J. Frank for generously allowing us the use of her Balzers 301 apparatus to perform the deep etching and rotary shadowing experiments. This work was supported by an MDA Jerry Lewis Neuromuscular Research Center grant.

References

1. Bulger, R. 1965. The shape of rat kidney tubular cells. *Am. J. Anat.* **116**:239–256
2. Costello, M.J., Corless, J.M. 1978. The direct measurement of temperature changes within freeze-fracture specimens during rapid quenching in liquid coolants. *J. Microsc. (Oxford)* **112**:17–37
3. Dubochet, J., Lepault, J., Freeman, R., Berriman, J.A., Homo, J.-C. 1982. Electron microscopy of frozen water and aqueous solutions. *J. Microsc. (Oxford)* **128**:219–237
4. Ernst, S.A., Schreiber, J.H. 1981. Ultrastructural localization of $(Na^+ + K^+)$-ATPase in rat and rabbit kidney medulla. *J. Cell Biol.* **91**:803–813
5. Goodenough, U.W., Heuser, J.E. 1982. Substructure of the outer dynein arm. *J. Cell Biol.* **95**:789–815
6. Heuser, J.E. 1983. Structure of the myosin cross bridge lattice in insect flight muscle. *J. Mol. Biol.* **169**:123–154
7. Heuser, J.E. 1983. A new method for visualizing freeze-dried molecules absorbed on mica. *J. Mol. Biol.* **169**:155–195
8. Heuser, J.E., Cooke, R. 1983. Actin-myosin interactions visualized by the quick-freeze, deep-etch replica technique. *J. Mol. Biol.* **169**:97–122
9. Heuser, J.E., Kirschner, M.W. 1980. Filament organization revealed in platinum replicas of freeze-dried cytoskeletons. *J. Cell Biol.* **86**:212–234
10. Heuser, J.E., Salpeter, S.R. 1979. Organization of acetylcholine receptors in quick-frozen, deep-etched, and rotatory-replicated torpedo postsynaptic membranes. *J. Cell Biol.* **82**:150–173
11. Hirokawa, N., Heuser, J.E. 1981. Quick-freeze, deep-etch visualization of the cytoskeleton beneath surface differentiations of intestinal epithelial cells. *J. Cell Biol.* **91**:399–409
12. Kyte, J. 1976. Immunoferritin determination of the distribution of $(Na^+ + K^+)$-ATPase over the plasma membranes of renal convoluted tubules. I. Distal segment. *J. Cell Biol.* **68**:287–303
13. Kyte, J. 1976. Immunoferritin determination of the distribution of $(Na^+ + K^+)$-ATPase over the plasma membranes of renal convoluted tubules. II. Proximal segment. *J. Cell Biol.* **68**:304–318
14. Mahanty, J., Ninhem, B.W. 1976. Calculations and comparison of theory with experiments. *In:* Dispersion Forces. Chapter 3, pp. 66–95. Academic, New York

15. Miller, M., Revel, J.P. 1974. Scanning electron microscopy of the apical, lateral and basal surfaces of transporting epithelia in mature and embryonic tisues. *In:* Scanning Electron Microscopy, Part III. O.M. Johari and L. Corben, editors. pp. 549–555. ITT Research, Chicago, Illinois
16. Pease, D.C. 1955. Fine structure of the kidney seen by electron microscopy. *J. Histochem. Cytochem.* **3**:295–308
17. Pease, D.C. 1956. Infolded plasma membranes found in epithelia noted for their water transport. *J. Biophys. Biochem. Cytol.* **2**(Suppl.):203–208
18. Pease, D.C. 1973. Glycol methacrylate copolymerized with glutaraldehyde and urea as an embedment retaining lipids. *J. Ultrastruct. Res.* **45**:124–148
19. Root, D.J., Heuser, J.E. 1982. Surface of rod photoreceptor disk membranes: Integral membrane components. *J. Cell Biol.* **98**:487–500
20. Ruska, H., Moore, D.H., Weinstock, J. 1957. The base of the proximal convoluted tubule cell of rat kidney. *J. Biophys. Biochem. Cytol.* **3**:249–254
21. Sjostrand, F.S., Rhodin, J. 1953. The ultrastructure of the proximal convoluted tubules of the mouse kidney as revealed by high resolution electron microscopy. *Exp. Cell Res* **4**:426–456
22. Zampighi, G., Corless, J.M., Robertson, J.D. 1980. On gap junction structure. *J. Cell Biol.* **86**:190–198
23. Zampighi, G., Kyte, J., Freytag, J.W. 1984. Structural organization of $(Na^+ + K^+)$-ATPase in purified membranes. *J. Cell Biol.* **98**:1851–1864
24. Zampighi, G., Simon, S.A., Robertson, J.D., McIntosch, T.J., Costello, M.J. 1982. On the structural organization of isolated bovine lens fiber junctions. *J. Cell Biol.* **93**:175–189

Received 18 July 1985